Research Article

Real-Time Short-term Hydro-Thermal-Wind-Solar Power Scheduling Using Meta-Heuristic Optimization Technique

Sunimerjit Kaur[a*], Yadwinder Singh Brar[a], Jaspreet Singh Dhillon[b]

[a]*Department of Electrical Engineering, I.K. Gujral Punjab Technical University, Kapurthala 144603, Punjab, India*

[b]*Department of Electrical & Instrumentation Engineering, Sant Longowal Institute of Engineering and Technology, Sangrur 148106, Punjab, India*

ABSTRACT. In this paper, an advanced modus operandi named the α-constrained simplex method (*ACSM*) is deployed to resolve a real-time hydro-thermal-wind-solar power scheduling problem. *ACSM* is an updated articulation of the Nonlinear Simplex Method (*SM*) of Nelder and Mead. It has been designed after interbreeding an ordinary *SM* with some other methods like-evolutionary method, α-constrained method, etc. To develop this technique three alterations in the *SM* are adopted (i) α-level differentiation, (ii) mutations of the worst point, and (iii) the incorporation of multi-simplexes. A real-time multi-objective hydro-thermal-wind-solar power scheduling problem is established and optimized for the Kanyakumari (Tamil Nadu, India) for the 18th of September of 2020. Four contrary constraints are contemplated for this case study (i)fuel cost and employing cost of wind and solar power system, (ii) NO_x emission, (iii) SO_2 emission, and (iv) CO_2 emission. The fidelity of the projected practice is trailed upon two test systems. The first test system is hinged upon twenty-four-hour power scheduling of a pure thermal power system. The values of total fuel cost, NO_xemission, SO_2emission, and CO_2emission are attained as 4707.19$/day, 59325.23 kg/day, 207672.70 kg/day, and 561369.20 kg/day, respectively. In the second test system, two thermal generators are reintegrated with renewable energy resources (RER) based power system (hydro, wind, and solar system) for the same power demands. The hydro, wind, and solar data are probed with the Glimn-Kirchmayer model, Weibull Distribution Density Factor, and Normal Distribution model, respectively. The outturns using *ACSM* are contrasted with the *SM* and evolutionary method(*EM*). For this real-time hydro-thermal-wind-solar power scheduling problem the values of fuel cost, NO_x emission, SO_2 emission, and CO_2 emission are shortened to 1626.41 $/day, 24262.24 kg/day, 71753.80 kg/day, and 196748.20 kg/day, respectively for the specified interval using *ACSM* and with *SM*, these values are calculated as 1626.57 $/day, 24264.67 kg/day, 71760.98 kg/day, 196767.68 kg/day, respectively. The results for the same are obtained as 1626.74 $/day, 24267.10 kg/day, 71768.15 kg/day, 196787.55 kg/day, respectively, by using *EM*. The values of the operating cost of the solar system, wind system, total system transmission losses, and computational time of test system-2 with *ACSM*, *SM*, and *EM* are evaluated as 8438.76 $/day, 19017.42 $/day, 476.69 MW/day & 15.6 seconds; 8439.61 $/day, 19019.33 $/day, 476.74 MW/day and 16.8 sec; and 8447.20 $/day, 19036.43 $/day, 477.17 MW/day and 17.3 sec, respectively. The solutions portray the sovereignty of *ACSM* over the other two methods in the entire process.

Keywords: Boundary-mutations, Multi-simplexes, Constrained-optimization, Uncertainty Cost, Hydro-Thermal-Wind-Solar Power Scheduling

1. Introduction

India is the third highest manufacturer and consumer of electricity in the world ("List of Countries by Electricity Production," n.d.) & ("Electricity Sector in India," n.d.). Its installed capacity up-to 30th of September of 2020 is 373.00 GW. About 36.17 % of generated power is from RER ("Renewable Energy in India," n.d.). India has projected a target to generate about 40 % of its total power generation from RER up-to 2030 (Ministry of New and Renewable Energy, 2019-20) in the Paris Climate Agreement.

RER, such as hydro, wind, solar, biomass, etc. have significant potential in India. In many parts of the country, more than one RER are accessible. Kanyakumari (Tamil Nadu, India) is one such place. India's biggest wind farm is instated here. Solar and hydro energies also have substantial prospects in this southernmost segment of the country.

In the past, Dasgupta and co-workers (2020) worked on power flow-based hydro-thermal-wind scheduling of hybrid power system using the sine cosine algorithm. The sine-cosine algorithm was employed to minimize fuel emission and generation cost. Dhillon *et al.* (2002) suggested fuzzy decision-making in stochastic multi-objective short-term hydrothermal scheduling. Nguyen *et al.* (2020) stated optimal scheduling of large-scale wind-

---
[*]Corresponding author: sunimerriar@yahoo.co.in(Sunimerjit Kaur)

hydro-thermal systems with a fixed-head short-term model. Ansari *et al.* (2020) suggested the consideration of the uncertainty of hydrothermal wind and solar-based DG. The researchers relied upon renewable energy assets to lower down the usage of fossil fuels as the basic source of ecological natural impurities. Vaderobli *et al.* (2020) developed optimization under uncertainty to reduce the cost of energy for parabolic trough solar power plants for different weather conditions. Das *et al.* (2018) presented fixed head short-term hydrothermal scheduling in presence of solar and wind power.They employed a point estimate method to model the unreliability of renewable sources. Mohamad *et al.* (2019) demonstrated a hybrid optimization technique for short-term wind-solar-hydrothermal generation scheduling. Narang *et al.* (2014) developed scheduling short-term hydrothermal generation using the predator-prey optimization technique. Ji *et al.* (2021) worked on an enhanced Borg algorithmic framework for solving the hydro-thermal-wind co-scheduling problem. They proposed the HTW-CS for constraint-handling. Biswas *et al.* (2017) worked on optimal power flow solutions incorporating stochastic wind and solar power. Saxena and Ganguli (2015) analyzed solar and wind power estimation and economic load dispatch using the firefly algorithm. Liaquat *et al.* (2021) presented the application of a dynamically search space squeezed modified Firefly Algorithm to a novel short-term economic dispatch of multi-generation systems. They used the fractional integral polynomial model and autoregressive integrated moving average model.Tan *et al.* (2019) suggested optimal scheduling of hydro-PV-wind hybrid system considering CHP and BESS coordination. Brar *et al.* (2005) stated fuzzy satisfying multi-objective generation scheduling based on simplex weightage pattern search. Reddy et al. (2016) elaborated the optimal operation of micro-grid using hybrid differential evolution and harmony search algorithm. Li and Kuri (2005) developed generation scheduling in a system with wind power. Naversen *et al.* (2020) presented hydrothermal scheduling in the continuous-time framework. The continuous-time framework was adapted to model adaptable hydropower resources associating with slow-ramping thermal power generators to minimize the operation cost of the hydrothermal system. Panda and Tripathy (2016) gave a solution of a wind integrated thermal generation system for environmental optimal power flow using a hybrid algorithm. Correa-Jullian *et al.* (2020) worked on operation scheduling in a solar thermal system: A reinforcement learning-based framework. An easy and adaptable reinforcement learning tabular Q-learning structure was implemented to recognize the optimal schedules for a hot water solar system. Kayalvizhi and Kumar (2018) analyzed stochastic optimal power flow in presence of wind generations using a harmony search algorithm. Damodaran and Kumar (2018) demonstrated hydro-thermal-wind generation scheduling considering economic and environmental factors using heuristic algorithms. Rahimi *et al.* (2021) stated optimal stochastic scheduling of electrical and thermal renewable and renewable resources in the virtual power plant.The scheduling of resources contemplating the unreliability of electrical and thermal loads was conducted.Reddy (2017a) worked on optimal scheduling of wind-thermal power system using clustered adaptive teaching learning-based optimization. He *et al.* (2019) gave integrated scheduling

of hydro, thermal, and wind power with spinning reserve. They proposed SHADE based on an improved heterogeneous real and binary number distinct evolution algorithm. Hetzer *et al.* (2008) developed an economic dispatch model incorporating wind power. Dubey *et al.* (2015) worked on a hybrid flower pollination algorithm with a time-varying fuzzy selection mechanism for a wind-integrated multi-objective dynamic economic dispatch. Sukkiramathi and Seshaiah (2020) analyzed the wind power potential by the three-parameter Weibull distribution to install a wind turbine. Saxena and Rao (2015) compared Weibull parameters computation methods and analytical estimation of wind turbine capacity factor using a polynomial power curve model and did a case study of a wind farm.The capacity factor of wind turbines was analytically estimated through the design of probability of wind speed and power curve of wind turbines (instated at Soda site). Nagababu *et al.* (2015) evaluated wind resources in selected locations in Gujarat. Ma *et al.* (2017) demonstrated a power generation scheduling for wind-solar-thermal power long-distance consumption based on game-theory. Reddy (2017b) analyzed the optimization of renewable energy resources in hybrid energy systems. Kumar *et al.* (2019) established wind energy potential assessment by Weibull parameter estimation using a multiverse optimization method: A case study of the Tirumala region in India. Takahama and Sakai (2005) stated constrained optimization by applying the α-constrained method to the nonlinear simplex method with mutations.

In this paper, an elaborated meta-heuristic optimization technique named as - the *ACSM* is employed to resolve a real-time hydro-thermal-wind-solar power scheduling problem for Kanyakumari (Tamil Nadu, India). This technique is composed after applying three alterations in the common *SM* (i) implementing α- level comparisons, (ii) mutations of the worst points, and (iii) exerting multi-simplexes. It is developed after the fusion of many approaches – e.g. (i) *SM*, (ii) *EM*, and (iii) some other mathematical procedures like the α-constrained method. In the proposed method, multi-simplexes are formed around the initial points. The contrasted points are based on their constraint defying. The simplexes gently creep up towards the optimum solution during the iterations. The decision-making (DM) has an unspecified nature. Therefore, it is considered that DM has fuzzy targets. The objectives are assessed by inducing an analogous membership function. The validity of this method is confirmed on two test systems. The results are differentiated with *SM* and *EM*. The supremacy of *ACSM* over the other two techniques from which it is composed is depicted in the whole exercise. It is observed that *ACSM* is a stable, constructive, fast, explicit, and solid technique for constrained optimization.

2. Multi-objective Problem Formulation

Four constraints are scrutinized for the presented real-time hydro-thermal-wind-solar power scheduling problem. These clashing constraints are (i) cost (fuel cost and the employing cost of wind and solar power system), (ii) NO_x emission, (iii) SO_2 emission, and (iv) CO_2 emission. These constraints can be examined as:

2.1. Economy constraint

The thermal unit fuel cost, wind power cost, and solar power cost are appraised as an indispensable criterion for economic viability. The economy constraint for the optimization interval of the hydro-thermal-wind-solar power system is stated as (Dhillon *et al.* 2002; Biswas *et al.* 2017; Kothari and Dhillon 2011):

$$F_1 = \int_0^{T_m} \left(\sum_{i=1}^{gt} \left(a_{ti}P_{ti}^2(t) + b_{ti}P_{ti}(t) + c_{ti} \right) + \sum_{j=1}^{gw} w_{wj}(t) + \sum_{q=1}^{gs} w_{sq}(t) \right) dt \tag{1}$$

where:

- gt and gw are the number of thermal and wind generators, respectively
- gs is the number of solar units
- $P_{ti}(t)$ is the output power of the ith thermal generator for t^{th} interval, in MW
- a_{ti}, b_{ti} & c_{ti} are the cost coefficients of the ith thermal generator
- $w_{wj}(t)$ is the wind power cost of the jth wind generator for t^{th} interval
- $w_{sq}(t)$ is the solar power cost of the qth solar unit for t^{th} interval
- T_m is the total planning period

2.2. Environmental constraints

The emission and the cost curves can be directly related through a constant factor called emission rate per Mkcal for a specified grade and category of fuel. Therefore, in this paper, three thermal emissions-NO_x emission, SO_2 emission, and CO_2 emission are observed as the quadratic functions of thermal output power. The NO_x emission of the viewed period can be evaluated as (Kothari and Dhillon 2011):

$$F_2 = \int_0^{T_m} \left(\sum_{i=1}^{gt} \left(d_{1i}P_{ti}^2(t) + e_{1i}P_{ti}(t) + f_{1i} \right) \right) dt \tag{2}$$

where:

- d_{1i}, e_{1i} & f_{1i} are the coefficients of NO_x emission of the ith thermal generator

SO_2 emission for the observed interval can be given as (Kothari and Dhillon 2011):

$$F_3 = \int_0^{T_m} \left(\sum_{i=1}^{gt} \left(d_{2i}P_{ti}^2(t) + e_{2i}P_{ti}(t) + f_{2i} \right) \right) dt \tag{3}$$

where:

- d_{2i}, e_{2i} & f_{2i} are the coefficients of SO_2 emission of the ith thermal generator

CO_2 emission for the optimization interim can be obtained as (Kothari and Dhillon 2011):

$$F_4 = \int_0^{T_m} \left(\sum_{i=1}^{gt} \left(d_{3i}P_{ti}^2(t) + e_{3i}P_{ti}(t) + f_{3i} \right) \right) dt \tag{4}$$

where:

- d_{3i}, e_{3i} & f_{3i} are coefficients of CO_2 emission of the ith thermal generator

2.3. Hydro model

Insubstantial fuel cost is experienced during the operation of hydro units. The characteristics (input/output) of these units are conveyed by water discharge. According to the Glimn-Kirchmayer model, the variation of water discharge of the uth hydro generator for t^{th} interval is given as (Dhillon *et al.* 2002; Narang *et al.* 2014; Kothari and Dhillon 2011; El-Hawary and Ravindranath 1988):

$$Q_u(t) = K_1 \varphi(H)\tau(P_{hu}(t))m^3/h \tag{5}$$

where:

- φ and τ are the functions of water head and hydro-generations, respectively
- $P_{hu}(t)$ is an output of the uth hydropower unit for t^{th} interval, in MW
- K_1 is a constant

For a fixed effective head, $\varphi(H)$ becomes constant, therefore Eq. (5) can be reworded as (Dhillon *et al.* 2002; Narang *et al.* 2014; Kothari and Dhillon 2011):

$$Q_u(t) = K'\tau(P_{hu}(t)) \tag{6}$$

where:

- K' is the new constant structured by the product of K_1 and $\varphi(H)$

The hydroelectric power plants are constrained by the quantity of water accessible for the optimization period. It can be displayed as (Dhillon *et al.* 2002; Narang *et al.* 2014; Kothari and Dhillon 2011):

$$\int_0^{T_m} Q_u(t)dt = R_u, \qquad u = gt + 1, \dots gh \tag{7}$$

where:

- R_u is the predetermined volume of water available in m³

Water discharge for t^{th} interval is observed as the quadratic functions of hydro output power and stated as (Dhillon *et al.* 2002; Narang *et al.* 2014; Kothari and Dhillon 2011):

$$Q_u(t) = x_u P_{hu}^2(t) + y_u P_{hu}(t) + z_u, \\ u = gt + 1, \dots gh \tag{8}$$

where:

- x_u, y_u, and z_u are the discharge coefficients of the uth hydro unit
- gh is the number of hydro-generators

2.4. Wind model

Wind power generating systems have undergone an enormous enlargement in the world. Its prime downside is the unpredictability of wind power generation which brings on complexity in the governing of power systems. The unsure wind data is observed in the Weibull Distribution Density Factor, in this paper. The Probability Density Function (PDF) of wind speed can be given as (Biswas *et al.* 2017; Reddy *et al.* 2016; Hetzer *et al.* 2008):

$$f_{pdf} = \left(\frac{k}{c}\right)\left(\frac{v}{c}\right)^{k-1} exp\left[-\left(\frac{v}{c}\right)^k\right], \qquad (0 \leq v \leq \infty) \qquad (9)$$

where:
- v and c are the annual average wind speed and the scale factor, respectively, in m/s
- k is the shape factor

The Weibull shape factor displays the width of wind speed distribution. This dimensionless factor shows the effect of topology on wind speed distribution. The shape factor can be expressed as (Biswas *et al.* 2017; Saxena and Ganguly 2015; Singal 2009):

$$k = \left(\frac{\sigma}{v_m}\right)^{-1.086} \qquad (10)$$

where:
- v_m and σ are the mean and mode speeds of wind, respectively, in m/s

The scale factor is can be obtained as (Biswas *et al.* 2017; Saxena and Ganguly 2015; Singal 2009):

$$c = \frac{v_m}{\Gamma\left(1 + \frac{1}{k}\right)} \qquad (11)$$

The Gamma Function $\Gamma(x)$ is commonly defined through an intersecting improper integral. It can be calculated as (Biswas *et al.* 2017):

$$\Gamma(x) = \int_0^\infty e^{-t} t^{x-1} dt \qquad (12)$$

The PDF of wind power can be stated as (Saxena and Ganguly 2015; Kaur *et al.* 2020a):

$$f(Pvj(t)) = \begin{cases} \left(\frac{k\, I_j v_{nj}}{c}\right)\left(\frac{(1+\rho_j I_j)v_{nj}}{c}\right)^{k-1} exp\left[-\left(\frac{(1+\rho_j I_j)v_{nj}}{c}\right)^k\right] & ; for\ 0 < v_p(t) < v_{rj} \\ 1 - exp\left[-\left(\frac{v_{rj}}{c}\right)^k\right] + exp\left[-\left(\frac{v_{0j}}{c}\right)^k\right] & ; for\ v_p(t) = 0 \\ exp\left[-\left(\frac{v_{rj}}{c}\right)^k\right] - exp\left[-\left(\frac{v_{0j}}{c}\right)^k\right] & ; for\ v_p(t) = v_{rj} \end{cases} \qquad (13)$$

where:
- v_{nj}, v_{rj}, and v_{oj} are the cut-in speed, the rated speed, and the cut-out speed, respectively, of the jth wind generator in m/s
- $v_p(t)$ is the operating wind speed for t^{th} interval, in m/s

- $\rho_j = \frac{v_p(t)}{v_{rj}}$. It is the ratio of operating wind speed to the rated wind speed for t^{th} interval
- $I_j = \frac{(v_{rj} - v_{nj})}{v_{nj}}$. It is the ratio of the difference between the rated speed and cut-in speed to cut-in speed, for t^{th} interval

$$Pvj(t) = \begin{cases} 0 & ; for\ v_p(t) < v_{nj}\ and\ v_p(t) > v_{oj} \\ \dfrac{P_{wrj}\,(v_p(t) - v_{nj})}{(v_{rj} - v_{nj})} & ; for\ v_{nj} < v_p(t) < v_{rj} \\ P_{wrj} & ; for\ v_{rj} \leq v_p(t) \leq v_{oj} \end{cases} \qquad (14)$$

where:
- P_{wrj} is the rated power of the jth wind generator

At different wind velocities, the wind power available for the jth wind generator for t^{th} time interval can be obtained as displayed in Eq 14 (Reddy et al. 2016). Eq. 14 displays that the wind power available at the considered location depends upon operating wind speeds during the examined interval and the ratings of the jth wind generator.

The prophecy wind power may not invariably be equal to the available wind power because of unsettled actions

of wind. Therefore, the factual wind power cost is usually more than its predicted cost. When the available wind power is less than the organized wind power, the arranger has to a recompense penalty cost, called the overestimation cost. When the planned wind power is less than actual wind power, a fine is imposed on the operator for not using the available wind power, called underestimation cost. The direct cost function of the jth wind generator for t^{th} interval can be observed as (Reddy 2017a; Hetzer et al. 2008; Dubey *et al.* 2015):

$$z_{dwj}(t) = z_{w1j}P_{wj}(t) \qquad (15)$$

where:
- z_{w1j} is the coefficient of the direct cost of the jth wind generator

$$z_{owj}(t) = z_{w2j} \int_0^{P_{wj(t)}} (P_{wj}(t) - Pvj(t))\, f(Pvj(t))\, d(Pvj(t)) \qquad (16)$$

where:
- z_{w2j} is the coefficient of overestimation cost of the jth wind generator.

$$z_{uwj}(t) = z_{w3j} \int_{P_{wj(t)}}^{P_{wrj}} (Pvj(t) - P_{wj}(t))\, f(Pvj(t))\, d(Pvj(t)) \qquad (17)$$

where:
- z_{w3j} is the coefficient of underestimation cost of the jth wind generator

The total operating wind power cost of the system is equal to the sum of the direct cost, the overestimation cost, and the underestimation cost.

2.5. Model of solar units (PV)

Solar energy is harnessed from the sun in the form of radiations, using a range of technologies. The intensity of solar irradiance fluctuates with the geography and climate of a locale. In this paper, the undetermined solar data is surveyed by the Normal Distribution Model. The Probability Density Function (PDF) of insolation for t^{th} interval can be examined as (Dukkipati *et al.* 2019; Kaur *et al.* 2020b):

$$Fs(I_T(t)) = \frac{e^{\frac{-(I_T(t)-m)^2}{2s^2}}}{s\sqrt{2\pi}} \qquad (18)$$

where:
- $I_T(t)$ and m are the solar irradiances for t^{th} interval and the mean of solar irradiance over the year, respectively in kWh/m²/day
- s is the standard deviation of solar prominence in kWh/m²/day.

The power available of the qth solar unit for t^{th} interval can be stated as (Tan *et al.* 2019):

$$Pavq(t) = P_{srq} \frac{\left(1 + k_T\left(T_{op}(t) - T_{rq}\right)\right)I_s(t)}{I_{max}} \qquad (19)$$

where:

- $P_{wj}(t)$ is the scheduled wind power of the jth wind generator for t^{th} interval

The overestimation cost function of the jth wind generator for t^{th} interval is observed as (Reddy 2017a; Kayalvizhi and Kumar 2018; Hetzer *et al.* 2008; Dubey *et al.* 2015):

The underestimation cost function for t^{th} interval of the jth wind generator can be expressed as (Reddy 2017a; Hetzer *et al.* 2008; Dubey *et al.* 2015):

- $T_{op}(t)$ and T_{rq} are the operating temperatures for t^{th} interval and the reference temperature of the qth solar unit, respectively, in °C
- P_{srq} is the rated power of qth solar unit in MW
- k_T is the temperature coefficient in /°C
- I_{max} is the maximum value of solar irradiance that descends under standard situations, in kWh/m²/day

The entire solar radiation falls on a tilted flat collector depends upon (i) diffused sky radiation, (ii) diffused radiation reflected from the surface of the earth, and (iii) beam radiation. The solar irradiance fall on a tilted plane for t^{th} interval is evaluated as (Singal 2006; Kaur *et al.* 2021):

$$I_s(t) = \frac{I_T(t)[\cos(\emptyset - g)\cos\delta\,\cos\omega + \sin(\emptyset - g)\sin\delta]}{(\cos\delta\cos\omega\cos\emptyset + \sin\emptyset\cos\delta)} \qquad (20)$$

where:
- $\emptyset$ is topographical latitude in (°)
- g is the tilt angle of the solar collector in (°)
- δ is the declination of the sun in (°)
- ω is the angle of the hour in (°)
- $g = \emptyset \pm 15°$

The angle of the declination of the sun can be observed as (Singal 2006):

$$\delta = 23.45° \sin\left(\frac{360(284 + D)}{365}\right) \qquad (21)$$

where:
- D is the number of the day of the year

The operating cost of the solar power system is the sum of the direct cost, overestimation cost, and underestimation cost of the qth solar unit. The function of the direct cost of the qth solar unit for t^{th} interval can be examined as (Biswas *et al.* 2017):

$$\sum_{q=1}^{gs} z_{dsq}(t) = \sum_{q=1}^{gs} (S_{1sq} P_{sq}(t)) \qquad (22)$$

where:
- S_{1sq} is the coefficient of the direct cost of the qth solar unit
- $P_{sq}(t)$ is the scheduled power of the qth solar unit for t^{th} interval

The function of overestimation cost of the qth solar power unit for t^{th} interval is stated as (Biswas *et al.* 2017):

$$\sum_{q=1}^{gs} z_{osq}(t) = \sum_{q=1}^{gs} \left(S_{2sq} \left(P_{sq}(t) - Pavq(t) \right) \right) Fs(I_T(t)) \qquad (23)$$

where:
- S_{2sq} is the coefficient of overestimation cost of the qth solar unit

The function of underestimation cost of the qth solar power unit for t^{th} interval can be observed as (Biswas *et al.* 2017):

$$\sum_{q=1}^{gs} z_{usq}(t) = \sum_{q=1}^{gs} \{ S_{3sq} (Pavq(t) - P_{sq}(t)) \} Fs(I_T(t)) \qquad (24)$$

where:
- S_{3sq} is the coefficient of the underestimation cost of the qth solar unit

The total employing cost of the qth solar unit for t^{th} interval can be examined as (Biswas *et al.* 2017):

$$\sum_{q=1}^{gs} W_{Sq}(t) = \sum_{q=1}^{gs} (z_{dsq}(t) + z_{osq}(t) + z_{usq}(t)) \qquad (25)$$

2.6. Multi-objective optimization problem

The multi-objective power scheduling problem of the hydro-thermal-wind-solar power system can be given as (Biswas *et al.* 2017; Saxena and Ganguly 2015; Kothari and Dhillon 2011; Mondal *et al.* 2013):

Minimize $[F_1, F_2, F_3, F_4]^{T_m}$

Subject to

$$\sum_{i=1}^{gt} P_{ti}(t) + \sum_{u=1}^{gh} P_{hu}(t) + \sum_{j=1}^{gw} P_{wj}(t) + \sum_{q=1}^{gs} P_{sq}(t) = P_D(t) + P_{Loss}(t) \qquad (26)$$

$$\int_0^{T_m} Q_u dt = R_u$$

$$P_{ti_{min}} \le P_{ti}(t) \le P_{ti_{max}}$$
$$0 \le P_{wj}(t) \le P_{wrj}$$
$$0 \le P_{sq}(t) \le P_{srq}$$
$$Q_{u_{min}} \le Q_u(t) \le Q_{u_{max}}$$

where:
- $P_D(t)$ and $P_{Loss}(t)$ are the system's power demand, and the transmission losses, respectively, for t^{th} interval, in MW
- $P_{ti_{min}}$ and $P_{ti_{max}}$ minimum and maximum limits of the output power of the ith thermal generator, respectively, in MW
- $Q_{u_{min}}$ and $Q_{u_{max}}$ are minimum and maximum limits of water discharge, respectively, of the uth hydro unit, in m^3/h

$$P_{LT}(t) = \sum_{i=1}^{gt} \left(\sum_{j=1}^{gt} P_{ti}(t) B_{TiTj} P_{tj}(t) \right) \qquad (27)$$

$$P_{LH}(t) = \sum_{i=1}^{gh} \left(\sum_{j=1}^{gh} P_{hi}(t) B_{hihj} P_{hj}(t) \right) \qquad (28)$$

$$P_{LW}(t) = \sum_{i=1}^{gw} \left(\sum_{j=1}^{gw} P_{wi}(t) B_{wiwj} P_{wj}(t) \right) \qquad (29)$$

$$P_{Ls}(t) = \sum_{i=1}^{gs} \left(\sum_{j=1}^{gs} P_{si}(t) B_{sisj} P_{sj}(t) \right) \qquad (30)$$

where:
- $P_{LT}(t)$, $P_{LH}(t)$, $P_{LW}(t)$, and $P_{LS}(t)$ are the transmission losses of the thermal system, the hydro system, the wind system, and the solar system, respectively, in MW, for the tth interval

Total transmission losses of the entire system for t^{th} interval can be observed as:

$$P_{Loss}(t) = P_{LT}(t) + P_{LH}(t) + P_{LW}(t) + P_{LS}(t) \qquad (31)$$

2.7. Transmission losses

The transmission losses of a power system can diversify from 5 to 15 of the total system load. It is, therefore, necessary to consider the transmission losses during the development of economic load dispatch schemes. The transmission losses of the short term hydro-thermal-wind-solar power system can be evaluated by using Kron's approximated loss formula having beta-coefficients and for the tth interval, it can be stated as (Kothari and Dhillon 2011):

3. Solution Methodology

ACSM is an updated elaboration of the Nonlinear Simplex Method (*SM*) of Nelder and Mead. It has been designed

after the integration of an ordinary *SM* with some other methods, like - mathematical methods, evolutionary method, α-constrained method, etc (Takahama and Sakai 2005).

A normal *SM* has many deficiencies therefore three remoldings have been inserted into it. An unconstrained optimization technique can be transfigured to a constrained optimization technique with the use of α-level comparisons. Here the preference is given to the satisfaction level over the value of the objective function.

In a customary *SM*, when simplex is contracted, a part of points around the partition of the feasible zone are overlooked, occasionally. Therefore, boundary mutations are inserted for probing the boundary of the feasible zone.

Sometimes simplex may lose affine self-reliance and can't reach the optimal solution. Therefore, multi-simplexes are used rather than a single simplex. The incorporation of mutation of the worst point and multi-simplexes also improve the perfection of the method.

3.1. Assessment of α

To procure superior results for the problems, which have a very small feasible region, controlled values of α are required. Its values lie between (0–1). The values of the α, (using Eqs. (35-36)) can be observed as (Takahama and Sakai 2005):

$$\alpha(T) = \begin{cases} \frac{1}{2}\left(max\left(\mu_d(A^i)\right) + \frac{1}{M}\sum_{i=1}^{M}\mu_d(A^i)\right) & ; T = 0 \\ (1-\beta)\alpha(T-1) + \beta & ; 0 < T \leq \frac{T_{max}}{2} \text{ and } (T \bmod T_\alpha) = 0 \\ \alpha(T-1) & ; 0 < T \leq \frac{T_{max}}{2} \text{ and } (T \bmod T_\alpha) \neq 0 \\ 1 & ; T > \frac{T_{max}}{2} \end{cases} \tag{32}$$

where:
- T and T_{max} are the number of iteration and the maximum iterations, respectively
- β and T_α are controlling parameters of α
- M is the number of search points

3.2. Algorithm of α-constrained Simplex Method

Assume 'Sp' is the search space of feasible solutions, $f(y)$ is an objective function, and $y = [A^1, A^2, ..., A^m]^T$ is an m-dimensional vector of decision variables. Put expansion factor $E > 1$, contraction factor $L \in (0,1)$, mutation rate $M_r \in (0-1)$, tolerance limit $\varepsilon = 0.001$, $\beta = 0.03$, and $T_\alpha = 50$. The algorithm of *ACSM* can be perceived as (Takahama and Sakai 2005):

1. Initialize the population, $M (> m + 1)$ for multi-simplexes. M number of search points are compulsory to construct one simplex, therefore, to formulate multi-simplexes more than M points are necessary.
2. Find A^l (the most desirable point), A^h (least desirable point), and A^s (second-worst point), from the following equations:

$$A^l = arg\ min_i\ f(y^i)$$

$$A^h = arg\ max_i\ f(y^i)$$

$$A^s = arg\ max_{i \neq h}\ f(y^i)$$

3. Generate the random number R and recondition A^h as:

$$A^h = \begin{cases} A^l + R(A^h - A^l) & ; R \geq M_r \tag{33} \\ A^h - R(A^h - A^l) & ; \text{ Else} \tag{34} \end{cases}$$

4. Drop the least desirable point and frame the initial simplex with $m + 1$ points. Then the centroid can be evaluated as:

$$A^0 = \frac{1}{m+1}\sum_{\substack{i=1 \\ i \neq h}}^{m+1} A^i$$

5. Calculate the value of α using Eqs. (32, 35 & 36) and then reflect the most desirable point of the simplex about the centroid to obtain reflected point A^r as:

$$A^r = (1 + \alpha)A^0 - \alpha A^h$$

6. If $f\left(A^r, \mu_d(A^r)\right) <_\alpha f\left(A^l, \mu_d(A^l)\right)$, i.e. the reflected point is better than the most desirable point, then the reflection is reckoned to have snared the simplex to a superior zone in the search space. It is called the expansion process. Therefore, go to step 7, else go to step 8.

7. Expansion is executed towards the reflected point from the centroid. Evaluate the expansion point A^e as:

$$A^e = EA^r + (1 - E)A^0$$

If $f\left(A^e, \mu_d(A^e)\right) <_\alpha f\left(A^l, \mu_d(A^l)\right)$, i.e. the expansion point is better than the most desirable point then A^h is replaced by A^e, else A^h is replaced by A^r, and go back to step 2.
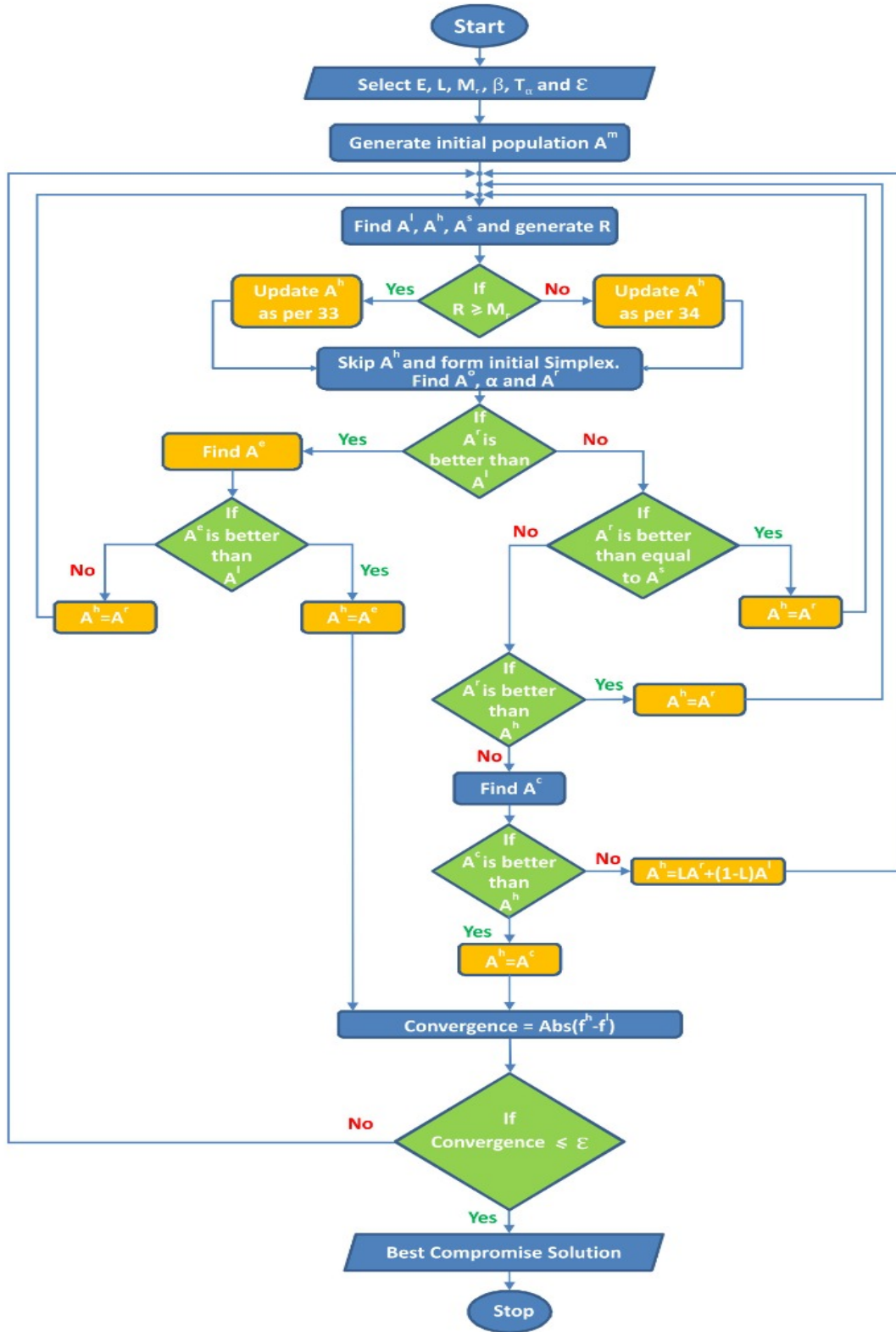
Fig. 1 Flow Chart of *ACSM*

8. If $f\left(A^r, \mu_d(A^r)\right) \leq_\alpha f\left(A^s, \mu_d(A^s)\right)$, ie. the reflected point is better than equal to the second-worst point, then it means that the reflection is contemplated to have carried the simplex towards the inferior zone. Therefore, contraction operation takes place. The proportion of contraction is regulated by the contraction factor *L*. Now, replace A^h with A^r and go back to step 2, else go to step 9.

9. If $f\left(A^r, \mu_d(A^r)\right) <_\alpha f\left(A^h, \mu_d(A^h)\right)$, ie. the reflected point is better than the least desirable point then

A^h is replaced by A^r. The direction of contraction is from the centroid towards the reflected point.

10. Find the contraction point A^c as:

$A^c = LA^h + (1 - L)A^0$

If $f(A^c, \mu_d(A^c)) <_\alpha f(A^h, \mu_d(A^h))$, i.e. the contraction point is better than the least desirable point then A^h is replaced by A^c, else renovate A^h as:

$A^h = LA^h + (1 - L)A^l$

and go to step 2.

11. If abs $(f^l - f^h) \leq \varepsilon$ then go to step 12, otherwise go to step 2.
12. Stop

3.3. Flowchart

Fig. 1 represents the flowchart that explains the entire process of *ACSM* as discussed earlier.

3.4. Effect of ACSM parameters

(i) The mutation rate of the worst points:

The mutations are introduced to find the solutions encircling the boundary of the feasible area and to command the convergence speed of the explored points. If the mutations are conducted with a high mutation rate then the number of assessments of the constraints will increase and therefore the speed of the algorithm may decrease (Takahama and Sakai 2005).

(ii) The number of search points:

The number of surveyed points regulates the variation of investigated points and also manages the convergence speed of the search procedure. If this value is very less, then even with a high convergence speed, the variation sets off low and the inspected points repeatedly coincide to a local optimal. If this value is too high, then the convergence speed decreases, and therefore the explored points can't outstretch the global optimal (Takahama and Sakai 2005).

(iii) The value of β:

The feasible region can be enlarged by pacifying the value of α and can be brought down to the initial feasible region by putting the value of α equal to 1. The value of β regulates the speed of α. If the value of β is small, α reaches 1 slowly. Therefore, there is a low probability of convergence of the search point to a local optimum. If the value of β is very less then a large region can be searched by the search points. It includes the infeasible area which reduces the search proficiency (Takahama and Sakai 2005).

(iv) The contraction factor:

It controls the convergence speed of search criteria. If it is small, the inspected points reach their centroid quickly. The search points even with high convergence speed may converge to a local optimal omitting the global optimal. If it is too high, the possibility of convergence to local optimal is low. The convergence speed is low but the inspected points may not reach the global optimum, in this case (Takahama and Sakai 2005).

4. Decision-Making

The decision-making has an unspecified temperament and indistinct aims for the objective functions. These targets are tuned by setting up their membership functions. Their values range from $0 - 1$. The merit 0 of membership function stipulates aversion and value 1 specifies absolute affinity. It can be stated as (Kothari and Dhillon 2011):

$$\mu(f^i) = \begin{cases} 1 & ; f^i \leq f_{min}^i \\ \dfrac{f_{max}^i - f^i}{f_{max}^i - f_{min}^i} & ; f_{min}^i < f^i < f_{max}^i \quad (i = 1,2,\dots,M) \\ 0 & ; f^i \geq f_{max}^i \end{cases} \quad (35)$$

where:

- f^i is the objective-function
- f_{max}^i and f_{min}^i are maximum and minimum values of the objective function, respectively

The Fuzzy Cardinal Priority Ranking or the membership function of non-dominated outturns to a fuzzy set can be given as (Kothari and Dhillon 2011):

$$\mu_d^k = \frac{\sum_{i=1}^M \mu(f_k^i)}{\sum_{k=1}^K \sum_{i=1}^M \mu(f_k^i)} \quad (36)$$

where:

- K is the number of non-dominated results

5. Prospects of Renewable Energy in Kanyakumari (Tamil Nadu, India)

Kanyakumari is positioned at 8.088306° north 77.538452° east, which is the southernmost extremity of India (NCERT India," 2020-21). It owns plentiful RER (like-hydro, wind, solar, etc.). Its hydroelectric power projects, e.g. Kodayar Dam-I & II have 60 MW & 40 MW installed capacities, respectively ("Tamil Nadu Generation and Distribution Corporation Limited").

Kanyakumari possesses elevated wind speeds owing to its presence at sea-shores. India's biggest wind farm (at Muppandal) of 1500 MW installed capacity is inducted here ("Muppandal Wind Farm," n.d.). Figure 2 depicts the PDF (unit-less) of wind speeds during the perused period (18th of September of 2020) of Kanyakumari, which is calculated from Eq. (9). It shows that the probability of wind speed is high (about 0.06) during the night (9 PM to 7 AM) and goes on decreasing (about 0.05) with the rise of the sun (from 7 AM to 8 PM). Fig. 3 shows the PDF of solar irradiance during 24 hours of 18th of September of 2020 of Kanyakumari, which is evaluated using Eq. (18). Up to 9 AM the solar panel doesn't receive sufficient sun's radiations, therefore its PDF is found zero during this time. Its value is maximum (more than 1), from 10 AM to 11 AM. After that its value went down and rose again after 2 PM. It becomes zero again after 5 PM.
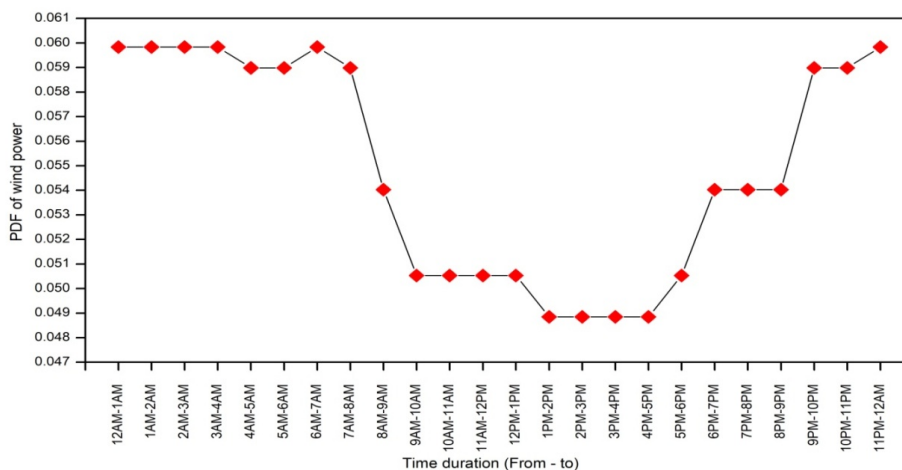
Fig. 2 Variation of PDF of wind power with the time of the Kanyakumari (Tamil Nadu, India)
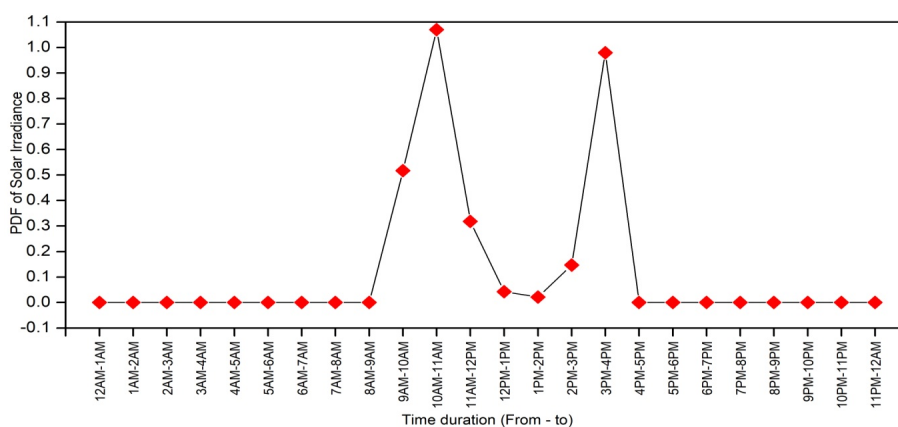
Fig. 3 Variation of PDF of solar irradiance with the time of the Kanyakumari (Tamil Nadu, India)

$$Q_1(t) = 0.0000219427P_{h1}^2 - 0.00025709P_{h1} + 1.742333 m^3/h \tag{37}$$

$$R_u = 72.4797 \, m^3 \tag{38}$$

6. Test Systems

In this paper, a real-time short-term multi-objective hydro-thermal-wind-solar power scheduling problem for Kanyakumari (Tamil Nadu, India) is constructed and it is optimized for the 18th day of September of 2020. To exemplify the eminence of the recommended technique, the following two test systems have been examined with the aid of the FORTRAN 90 computer programming language. These test systems are classified as:
   (i) Power scheduling of a pure thermal system
   (ii) Power scheduling of a hydro-thermal-wind-solar power system

6.1. Test system 1

It is worked out for four thermal generators power system. A 24 hour multi-objective thermal power scheduling problem is assessed by using *ACSM*, which can satisfy economic and emission objectives, concurrently. Fuel costs, NO_x emission, SO_2 emission, and CO_2 emission functions of four thermal generators are tabulated in Table 1. The minimum and maximum generation

restrictions for each thermal generator are contemplated as 10 MW and 250 MW, respectively.

6.2 Test System 2

This structure is encompassed around the scheduling of a coordinated hydro-thermal-wind-solar power system. It embodies two thermal generators, one hydro unit, one wind generator/farm, and one solar unit. The rate of discharge of hydro-generating station is obtained by Glimn-Kirchmayer model using Eqs. (5–8). The average annual data, as well as 24 hour data of wind farm/generator and solar power system, is looked over for the 18th of September of 2020 for Kanyakumari (Tamil Nadu, India). The wind character is surveyed by Weibull Distribution Density Factor using Eqs. (9–17) and solar irradiances are studied with the Normal Distribution Model by using Eqs. (18–25). Wind farm/generator and the solar unit parameters are ordered in Table 2. The shape factor 'k' is gained from Eq. (10), which is established as 1.4005. The scale factor 'c' is investigated by Eq. (11–12) and its value is observed as c = 8.23 m/s for Kanyakumari for the viewed duration. The water discharge rate is given by Eqs. (37–38).

Table 1

The characteristic fuel cost, NO_x emission, SO_2 emission, and CO_2 emission functions of four thermal generators

Fuel cost ($/h) equations	NO_xemission (kg/h) equations
$F_{11}=0.000018292P_{t1}^2(t) + 0.112900944P_{t1}(t) + 3.729447760$	$F_{21}=0.006732P_{t1}^2(t) - 2.39928P_{t1}(t) + 610.2535$
$F_{12}=0.000027676P_{t2}^2(t) + 0.114675880P_{t2}(t) + 1.164633280$	$F_{22}=0.006323P_{t2}^2(t) - 0.38128P_{t2}(t) + 80.9019$
$F_{13}=0.000081097P_{t3}^2(t) + 0.094052024P_{t3}(t) + 2.747550880$	$F_{23}=0.006181P_{t3}^2(t) - 0.39077P_{t3}(t) + 50.3808$
$F_{14}=0.000052578P_{t4}^2(t) + 0.087180216P_{t4}(t) + 4.131380800$	$F_{24}=0.006483P_{t4}^2(t) - 0.79027P_{t4}(t) + 28.8249$
SO_2emission (kg/h) equations	**CO_2emission (kg/h) equations**
$F_{31}=0.000813P_{t1}^2(t) + 4.97641P_{t1}(t) + 165.3433$	$F_{41}=0.106409P_{t1}^2(t) - 12.73642P_{t1}(t) + 1819.625$
$F_{32}=0.001206P_{t2}^2(t) + 5.05928P_{t2}(t) + 51.3778$	$F_{42}=0.265110P_{t2}^2(t) - 61.01945P_{t2}(t) + 5080.148$
$F_{33}=0.003578P_{t3}^2(t) + 4.14938P_{t3}(t) + 121.2133$	$F_{43}=0.403144P_{t3}^2(t) - 121.9812P_{t3}(t) + 11381.070$
$F_{34}=0.002320P_{t4}^2(t) + 3.84624P_{t4}(t)+ 182.2605$	$F_{44}=0.140053P_{t4}^2(t) - 29.95221P_{t4}(t) + 3824.770$

Table 2

Parameters of wind farm and solar unit (PV)

Wind system variables	Specifications	Solar system variables	Specifications
The capacity of each wind farm (MW)	30	The capacity of each solar unit (MW)	30
Rated speed v_r (m/s)	15	The angle of tilt of solar collector (°)	20
Cut in velocity v_n (m/s)	3.5	Hour angle (°)	±15
Cut out velocity v_o (m/s)	25	Temperature coefficient (/°C)	$-4.7\,e^{-3}$
Coefficient of direct cost ($/kWh)	0.05	Coefficient of direct cost ($/kWh)	0.06
Coefficient of overestimation cost ($/kWh)	0.17	Coefficient of overestimation cost ($/kWh)	0.17
Coefficient of underestimation cost ($/kWh)	0.24	Coefficient of underestimation cost ($/kWh)	0.24

Table 3

The solution of power scheduling problem with four thermal generators of test system-1 using $ACSM$

Time interval (t)	$P_D(t)$ (MW)	$Pt_1(t)$ (MW)	$Pt_2(t)$ (MW)	$Pt_3(t)$ (MW)	$Pt_4(t)$ (MW)	$P_{Loss}(t)$ (MW)
1	455	116.25	116.28	116.37	116.35	9.75
2	425	108.56	108.38	108.46	108.56	8.51
3	415	105.89	105.92	105.78	105.91	8.11
4	407	103.70	103.74	103.78	103.85	7.79
5	400	101.94	101.91	101.86	101.86	7.52
6	420	107.05	107.16	107.10	107.06	8.29
7	487	124.55	124.70	124.52	124.61	11.16
8	604	155.23	155.29	155.22	155.33	17.14
9	665	171.44	171.50	171.49	171.40	20.79
10	675	174.14	174.10	174.14	174.23	21.42
11	695	179.53	179.46	179.41	179.36	22.71
12	705	182.09	182.25	182.13	182.08	23.38
13	580	149.04	148.93	149.00	148.92	15.81
14	605	155.70	155.72	155.57	155.63	17.23
15	616	158.60	158.61	158.62	158.53	17.86
16	653	168.28	168.32	168.28	168.26	20.05
17	721	186.35	186.38	186.38	186.49	24.44
18	740	191.46	191.57	191.42	191.43	25.75
19	700	180.91	180.78	180.85	180.76	23.05
20	678	174.92	174.97	174.87	174.91	21.61
21	630	162.21	162.28	162.24	162.33	18.68
22	585	150.42	150.26	150.35	150.28	16.10
23	540	138.57	138.44	138.42	138.39	13.71
24	503	128.77	128.85	128.73	128.87	11.91

7. Results of Test Systems

7.1. Test System 1

The power scheduling problem is optimized for 24 individual power demands (for each hour of the whole day). The fuel costs, NO_x emission, SO_2 emission, and CO_2 emission are appraised through Eqs. (1-4). Transmission losses are summed up with the help of Eqs. (27-31). Decision-making is executed by employing Eqs. (35–36). All the results using $ACSM$ are systematized in Tables 3 & Supplementary Table S1. The power demand is minimum (400 MW) for the 5th time interval. The values of total transmission losses, F_1, F_2, F_3 & F_4 for this period are 7.52 MW, 141.02 $/h, 2230.68 kg/h, 6222.85 kg/h, and 19857.97 kg/h, respectively. Whereas these values for the maximum power demand (740 MW during 18th interval), are obtained as 25.75 MW, 246.70 $/h, 2829.59 kg/h, 10882.88 kg/h, and 31315.98 kg/h, respectively. Test system-1 is then judged by SM and EM and outturns are charted in Table 7.
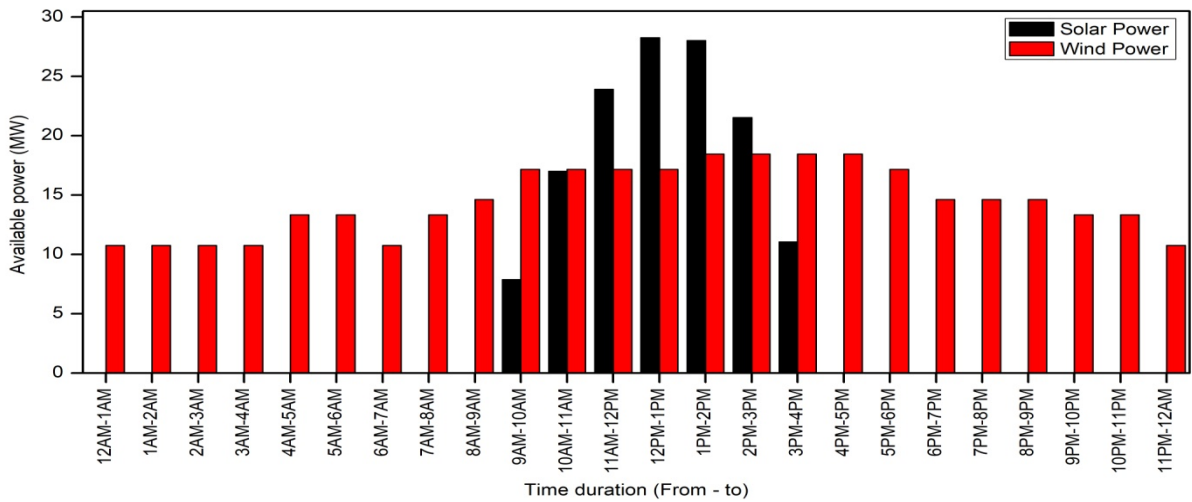
Fig. 4 Variation of available powers of wind and solar systems with the time of Kanyakumari (Tamil Nadu, India)
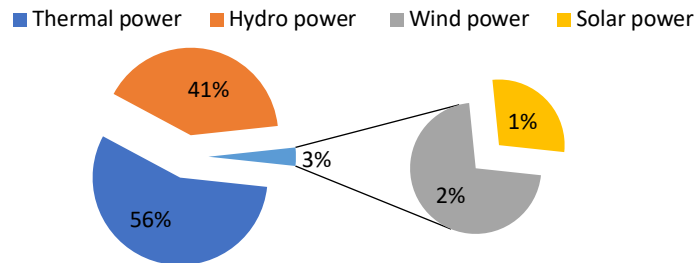
Fig. 5 Percentage of load shared by thermal, hydro, wind, and solar power systems for reviewed permutation of generating units at Kanyakumari (Tamil Nadu, India) using ACSM

7.2. Test system 2

The available wind power for each hour is gained from Eq. (14). Fig.4 displays the variation of available powers of wind and solar systems with the time of Kanyakumari (Tamil Nadu, India) for the considered day. It can be observed from the figure that the value of maximum available wind power is 18.46 MW/h, from 1 PM to 5 PM of the considered day. The minimum available wind power is observed as 10.75 MW/h from 12 AM to 4 AM, 6 AM to 7 AM, and 11 PM to 12 AM, respectively.

The available solar power is derived from Eq. (19) and its maximum value obtained is 28.25 MW/h from 12 PM to 1 PM and its minimum value is found as 7.88 MW/h from 9 AM to 10 AM of the stated day.

Table 4 represents the solution of power scheduling of hydro-thermal-wind-solar power system of test system-2 using *ACSM*. The total power demand is contemplated as 13904 MW. Whereas the total scheduled thermal power, hydropower, wind power, and solar power are 8072.15 MW/day, 5821.59 MW/day, 349.60 MW/day, and 137.95 MW/day, respectively for the considered permutation of generating units. Total transmission losses for the regarded period are quantified as 476.69 MW/day. The values of transmission losses and water discharge for maximum and minimum demands are 30.22 MW/h & 9.20 MW/h and 3.72 Mm³/h & 2.31 Mm³/h, respectively.

Fig. 5 depicts the percentage load shared by thermal, hydro, wind, and solar power systems during the studied period for the reviewed power demand and union of different power generating units, using *ACSM*.

Supplementary Table S2 depicts values of fuel cost, NO_x emission, SO_2 emission, and CO_2 emission of test system-2 obtained by *ACSM*. The values of $F_1, F_2, F_3 \& F_4$ for the maximum and minimum demands are 83.48 \$/h, 1094.88 kg/h, 3703.37 kg/h and 11945.48 kg/h and 48.60 \$/h, 967.44 kg/h, 2144.96 kg/h and 5092.03 kg/h, respectively.

Table 5 represents the values of operating costs of the solar system of test system-2 observed by *ACSM*. The solar unit starts delivering power after 9 AM up to 4 PM on the 18th of September of 2020 for the examined system when solar radiation and operating temperature reach the pre-specified values of the solar generating unit. The highest value of direct cost and total operating cost for the solar system is evaluated as 1728.90 \$/h and 1728.91 \$/h, respectively from 12 PM–1 PM for solar power generation of 28.25 MW.

For the wind power system the direct cost, the overestimation cost, and the underestimation cost are procured from Eqs. (15–17). Table 6 shows the values of operating costs of the wind system of test system-2 observed by *ACSM*. The values of the highest direct cost and total operating cost for wind system are 1009.12 \$/h and 1008.83 \$/h, respectively for 18.55 MW wind power generation for the 15th time interval.

The same problem is then solved with *SM* and *EM* and the outcomes of all the three methods are compared and tabulated in Table 7.

Table 4
Power scheduling of hydro-thermal-wind-solar power system (test system-2) using *ACSM*

Time interval (t)	$P_D(t)$(MW)	$Pt_1(t)$ (MW)	$Pt_2(t)$ (MW)	$Ph_1(t)$ (MW)	$Ps_1(t)$ (MW)	$Pw_1(t)$ (MW)	$P_{Loss}(t)$ (MW)	$Q_1(t)$ (Mm³/h)
1	455	132.37	132.33	191.46	0	10.55	12.091	2.50
2	425	123.17	123.19	178.25	0	11.00	10.52	2.39
3	415	120.12	120.09	173.91	0	10.50	10.02	2.36
4	407	117.66	117.66	170.38	0	10.80	9.62	2.34
5	400	114.94	114.93	166.36	0	13.00	9.20	2.31
6	420	121.05	121.04	175.13	0	13.50	10.17	2.37
7	487	142.22	142.23	205.52	0	11.00	13.90	2.62
8	604	177.95	177.91	256.61	0	13.55	21.42	3.12
9	665	196.48	196.52	283.01	0	14.75	25.91	3.43
10	675	199.00	199.02	286.70	0	17.00	26.57	3.47
11	695	205.04	205.04	295.15	0	17.25	28.12	3.58
12	705	208.54	208.51	300.15	0	17.00	29.04	3.64
13	580	166.67	166.67	240.58	7.75	17.20	18.92	2.95
14	605	171.24	171.29	247.02	17.20	18.50	19.97	3.02
15	616	172.55	172.57	248.86	24.00	18.55	20.29	3.04
16	653	182.72	182.71	263.42	28.25	18.40	22.67	3.20
17	721	204.30	204.27	294.11	28.00	18.50	28.04	3.56
18	740	212.70	212.71	306.03	21.55	17.00	30.22	3.72
19	700	204.12	204.08	293.85	11.20	14.75	27.88	3.56
20	678	200.77	200.82	289.15	0	14.50	27.01	3.50
21	630	185.61	185.60	267.51	0	14.55	23.23	3.24
22	585	171.89	171.84	247.98	0	13.50	20.04	3.03
23	540	157.80	157.84	227.83	0	13.25	17.00	2.82
24	503	147.14	147.17	212.62	0	11.00	14.85	2.68

Table 5
Values of operating costs of the solar system of test system 2 observed by *ACSM*

Time interval (t)	Direct cost ($/h)	Underestimation cost ($/h)	Overestimation cost ($/h)	Total operating cost of the solar system ($/h)
1–12	0	0	0	0
13	474.30	15.52	−11.03	478.79
14	1052.64	−17.35	12.33	1047.62
15	1468.80	−7.04	5.00	1466.76
16	1728.90	0.02	−0.012	1728.91
17	1713.60	0.13	−0.09	1713.64
18	1318.86	−0.65	0.46	1318.67
19	685.44	−3.68	2.62	684.37
20–24	0	0	0	0

Table 6
Values of operating costs of the wind system of test system 2 observed by *ACSM*

Time interval	Direct cost ($/h)	Underestimation cost ($/h)	Overestimation cost ($/h)	Total cost ($/h)
1	573.92	2.87	-2.04	574.75
2	598.40	-3.46	2.46	597.40
3	571.20	3.57	-2.54	572.23
4	587.52	-0.65	0.46	587.33
5	707.20	4.45	-3.16	708.49
6	734.40	-2.12	1.51	733.79
7	598.40	-3.46	2.46	597.40
8	737.12	-2.28	1.97	736.32
9	802.40	-1.51	1.08	801.96
10	924.80	2.01	-1.43	925.38
11	938.40	-0.96	0.68	938.12
12	924.80	2.01	-1.42	925.38
13	935.68	-0.37	0.26	935.57
14	1006.40	-0.44	0.31	1006.27
15	1009.12	-1.02	0.72	1008.83
16	1000.96	0.71	-0.50	1001.16
17	1006.40	-0.44	0.31	1006.27
18	924.80	2.01	-1.43	925.38
19	802.40	-1.51	1.08	801.96
20	788.80	1.66	-1.18	789.28
21	791.52	1.03	-0.73	791.82
22	734.40	-2.12	1.51	733.79
23	720.80	1.16	-0.83	721.14
24	598.40	-3.46	2.46	597.40

Table 7

Comparison of outcomes using *ACSM*, *SM*, and *EM*

S.No.	Output variables	ACSM	SM	EM
1	Total F_1 ($/day) of test system-1	4707.19	4707.67	4708.14
2	Total F_2 (kg/day) of test system-1	59325.23	59331.16	59337.10
3	Total F_3 (kg/day) of test system-1	207672.70	207693.47	207714.23
4	Total F_4 (kg/day) of test system-1	561369.20	561425.34	561481.47
5	Total F_1 ($/day) of test system-2	1626.41	1626.57	1626.74
6	Total F_2 (kg/day) of test system-2	24262.24	24264.67	24267.10
7	Total F_3 (kg/day) of test system-2	71753.80	71760.98	71768.15
8	Total F_4 (kg/day) of test system-2	196748.20	196767.68	196787.55
9	Total operating cost of the solar system ($/day)	8438.76	8439.61	8447.20
10	Total operating cost of the wind system ($/day)	19017.42	19019.33	19036.43
11	Total transmission losses (MW) of test system-2	476.69	476.74	477.17
12	Simulation time (seconds) of test system-2	15.6	16.8	17.3
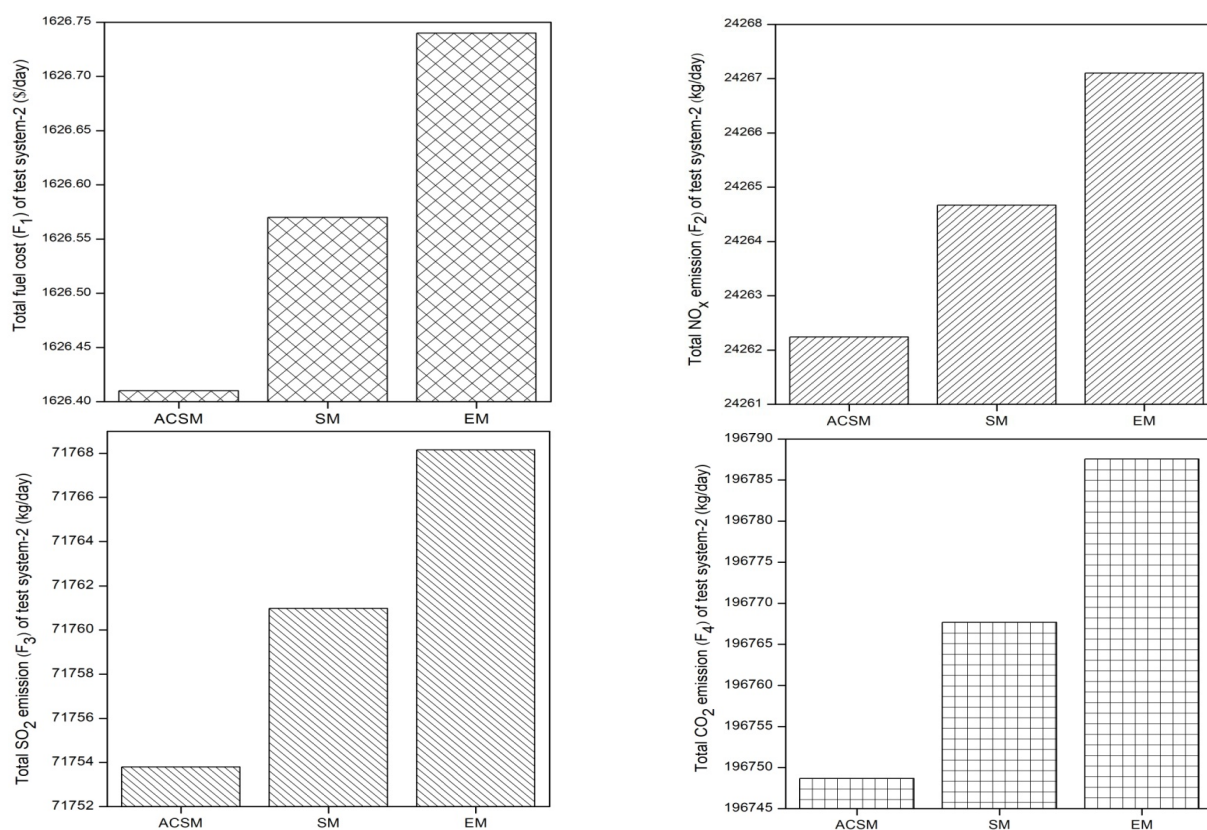
Fig. 6 Comparison of total fuel cost, NO_x emission, SO_2 emission, and CO_2 emission of test system-2 using *ACSM*, *SM* & *EM*

8. Comparisons

In an ordinary *SM* for 'm' objectives, *m+1* search points are explored to generate an initial simplex of non-zero volume. If *y = 1, 2……, m+1* and X^y- indicates each vertex of the initial simplex, then the least desirable point (worst point) of the initial simplex is searched. Then with the utilization of some fixed rules, a new simplex is constructed from the older one in such a manner that the search moves away from the least desirable point in the simplex. Whereas evolutionary algorithms operate by searching population enumeration to some extent, so that while the generation of newer individual solution, some of them would have superior genetic characteristics and

some would have inferior genetic characteristics. *ACSM* is composed with the amalgamation of these two methods along with the *α*-constrained method, in which a constraint satisfaction level is inserted to display how aptly the explored point satisfies the constraints. The performance of *SM*, *EM*, and *ACSM* is compared here.

In this paper, initially, a multi-objective thermal power scheduling problem is optimized in test system 1. Fuel cost, emissions, transmission losses, and simulation time are computed with *ACSM*. Then two thermal generators are integrated with (one each) generating units of hydro, wind, and solar system in test system 2. The operation of this hybrid system (for the Kanyakumari region of India

and the 18th of September of 2020) also takes in water discharge of the hydro system and operating cost of wind & solar systems. It is detected from Table 7 that now the values of total fuel cost, NO_x emission, SO_2 emission, and CO_2 emission are lowered from 4707.19 $/day, 59325.23 kg/day, 207672.70 kg/day, and 561369.20 kg/day to 1626.41 $/day, 24262.24 kg/day, 71753.80 kg/day, and 196748.20 kg/day, respectively, for the examined time interval.

The problem is optimized by using *ACSM*, and outcomes are weighed up with *SM* and *EM*. After contrasting the results observed by using *ACSM, SM*, and *EM*, it is revealed that *ACSM* brings out upper-level outturns than *SM* and *EM*. The values of fuel cost, NO_x emission, SO_2 emission, and CO_2 emission are calculated as 1626.57 $/day, 24264.67 kg/day, 71760.98 kg/day, 196767.68 kg/day, respectively, using SM. The results for the same are obtained as 1626.74 $/day, 24267.10 kg/day, 71768.15 kg/day, 196787.55 kg/day, respectively, by using *EM*.

The values of the operating cost of the solar system, wind system, transmission losses, and computational time with *ACSM, SM*, and *EM* are gained as 8438.76 $/day, 19017.42 $/day, 476.70 MW/day & 15.6 sec; 8439.61 $/day, 19019.33 $/day, 476.74 MW/day & 16.8 seconds; and 8447.20 $/day, 19036.43 $/day, 477.17 MW/day and 17.3 sec, respectively. It can be noticed that *ACSM* brings out the least transmission losses and computational time along with fuel cost, operating cost (wind and solar system), and emissions than the other two contemplated methods. Fig 6 shows the comparison of the total fuel cost, NO_x emission, SO_2 emission, and CO_2 emission of test system-2 using *ACSM, SM & EM*. It manifests that *ACSM* is advantageous to the other two methods from which it is produced, i.e. *SM* and *EM*. The comparisons prove that *ACSM* is a constructive, fast, explicit, and solid technique for constrained optimization. Also, it is not much affected by varying parameters.

9. Conclusion

India has a vast number of treasures of RER due to its magnificent topographical location. The fundamental aspects for employing RER-based power systems in the country are to upgrade energy surety, financial growth, moderate climate variation, boost up energy retrieve, etc.

Greater capital cost, intermittent nature of most of the RER, lack of pertaining land, storage potential, improper utilization schemes, etc. are the main constraints in the growth of this field. Therefore, currently, RER has very little contribution to the total basic commercial energy supply in India.

There is a vast scope for advancement in the RER-based power system in the countries like India. It is a well-renowned certainty that fossil fuel-based power systems are expensive, exhausting, and environment polluting. As proved in this paper, that the clever blending of the conventional power generation system with RER-based systems can bring about a revolution in the field of the electrical power system. These hybrid systems (such as hydro-thermal-wind-solar power systems) can reduce the shortcomings of conventional fossil fuel-relied structures as well as RER oriented systems. A large number of RER based power generating systems are already deployed at different places of India, but still, hybrid systems are very few. The Indian government is modeling strategies, programs and, enlightening atmosphere to push India to be one of the few masters of the most interesting markets of renewable energy in the world.

Sustainable electrical energy is required for the sustainable development of the world. Hybrid power systems like hydro-thermal-wind-solar power generating systems can corroborate reliable, reasonable, sustainable, and clean energy for the people.

Supplementary Material

The supplementary material for this article is:

Table S1
Values of fuel cost, NO_x emission, SO_2 emission, and CO_2 emission of four thermal generators of test system-1 achieved with *ACSM*

Table S2
Values of fuel cost, NO_x emission, SO_2 emission, and CO_2 emission of test system-2 obtained by *ACSM*

References

Ansari, M.M., Guo, C., Shaikh, M., Chopra N., Yang, B., Pan J., Zhu, Y., & Huang, X. (2020). Considering the uncertainty of hydrothermal wind and solar-based DG. *Alexandra Engineering Journal,* 59(6), 4211-4236; https://doi.org/10.1016/j.aej.2020.07.026

Biswas, P.P., Suganthan, P.N., & Amaratunga, G.A.J. (2017). Optimal power flow solutions incorporating stochastic wind and solar power. *Energy Conversion and Management,* 148, 1194-1207; https://doi.org/10.1016/j.enconman.2017.06.071

Brar, Y.S., Dhillon, J.S., & Kothari, D.P. (2005). Fuzzy satisfying multi-objective generation scheduling based on simplex weightage pattern search. *International Journal of Electrical Power & Energy Systems,* 27(7), 518-527; https://doi.org/10.1016/j.ijepes.2005.06.002

Correa-Jullian, C., Droguett, E.L., & Cardemil, J.M. (2020). Operation scheduling in a solar thermal system: A reinforcement learning-based framework. *Applied Energy,* 268, 114943; https://doi.org/10.1016/j.apenergy.2020.114943

Damodaran, S.K., & Kumar, T.K.S. (2018). Hydro-thermal-wind generation scheduling considering economic and environmental factors using Heuristic algorithms. *Energies,* 11(2), 353; https://doi.org/10.3390/en11020353

Das S., Bhattacharya, A., Chakraborty, A.K. (2018). Fixed head short-term hydrothermal scheduling in presence of solar and wind power. *Energy Strategy Reviews,* 22, 47-60; https://doi.org/10.1016/j.esr.2018.08.001

Dasgupta, K., Roy, P.K., & Mukherjee, V. (2020). Power flow based hydro-thermal-wind scheduling of hybrid power system using sine cosine algorithm. *Electric Power Systems Research,* 178, 106018; https://doi.org/10.1016/j.epsr.2019.106018

Dhillon, J.S., Parti, S.C., & Kothari, D.P. (2002). Fuzzy decision-making in stochastic multiobjective short-term hydrothermal scheduling. *IEE Proceedings - Generation, Transmission and Distribution,* 149(2), 191-200; https://doi.org/10.1049/ip-gtd:20020176

Dubey, H.M., Pandit, M., & Panigrahi, B.K. (2015). Hybrid flower pollination algorithm with time-varying fuzzy selection mechanism for wind integrated multi-objective dynamic economic dispatch. *Renewable Energy*, 83, 188-202; https://doi.org/10.1016/j.renene.2015.04.034

Dukkipati, S., Sankar, V., & Varma, P.S. (2019). Forecasting of solar irradiance using probability distributions for a PV system: a case study. *International Journal of Renewable Energy Research*, 9(2).

Electricity Sector in India. In Wikipedia. [Online] Available: https://en.wikipedia.org/wiki/Electricity_sector_in_India#:~:text=The%20national%20electric%20grid%20in,of%20India's%20total%20installed%20capacity. Accessed on 1 December 2020

El-Hawary, M.E., & Ravindranath, K.M. (1988). Optimal operation of variable head hydro-thermal systems using the Glimn-Kirchmayer model and the Newton-Raphson method. *Electric Power Systems Research,* 14(1), 11-22; https://doi.org/10.1016/0378-7796(88)90043-0

He, Z., Zhou, J., Sun, N., Jia, B., & Qin, H. (2019). Integrated scheduling of hydro, thermal and wind power with spinning reserve. *Energy Procedia,* 158, 6302-6308; https://doi.org/10.1016/j.egypro.2019.01.409

Hetzer, J., Yu, D.C., & Bhattarai, K. (2008). An economic dispatch model incorporating wind power. *IEEE Transactions on Energy Conversion,* 23(2), 603-611; https://doi.org/10.1109/TEC.2007.914171

Ji, B., Zhang, B., Yu, S.S., Zhang, D., & Yuan, X. (2021). An enhanced borg algorithmic framework for solving the hydro-thermal-wind co-scheduling problem. *Energy,* 218, 119512; https://doi.org/10.1016/j.energy.2020.119512

Kaur, S, Brar, Y.S., & Dhillon, J.S. (2020a). Multi-objective power scheduling of wind-thermal integrated system by using α-constrained simplex method.*International Conference on Smart Grid and Clean Energy Technologies (ICSGCE),* Kuching, Malaysia, pp. 112-119; https://doi.org/10.1109/ICSGCE49177.2020.9275653

Kaur, S., Brar, Y.S., & Dhillon, J.S. (2020b). Solar-thermal power scheduling by inserting α-constrained method to nonlinear simplex method with mutations.*International Conference on Smart Grid and Clean Energy Technologies (ICSGCE),* Kuching, Malaysia, pp. 27-34; https://doi.org/10.1109/ICSGCE49177.2020.9275629

Kaur, S, Brar, Y.S., & Dhillon, J.S. (2021). Optimal scheduling of solar-wind-thermal-integrated system using α-constrained simplex method. *International Journal of Renewable Energy Development,* 10(1), 47-59;https://doi.org/10.14710/ijred.2021.32245

Kayalvizhi, S., & Kumar, D.M.V. (2018). Stochastic optimal power flow in presence of wind generations using harmony search algorithm. *Proceedings of the 20th National Power Systems Conference,* Dec. 14-16, NIT Tiruchirappalli, India; https://doi.org/10.1109/NPSC.2018.8771822

Kothari, D.P., & Dhillon, J.S. (2011). *Power Systems Optimization.* 2nd ed. PHI, New Delhi, India.

Kumar, M.B.H., Balasubramaniyan, S., Padmanaban, S., & Holm-Nielsen, J.B. (2019). Wind energy potential assessment by Weibull parameter estimation using multiverse optimization method: a case study of Tirumala region in India. *Energies,* 12(11), 2158; https://doi.org/10.3390/en12112158

Li, F., & Kuri, B. (2005). Generation scheduling in a system with wind power. *2005 IEEE/PES Transmission & Distribution Conference & Exposition: Asia and Pacific,* Aug 18, Dalian, China, 1-6; https://doi.org/10.1109/TDC.2005.1547157

Liaquat, S., Fakhar, M.S., Kashif, S.A.R., Rasool, A., Saleem, O., Zia, M.F., & Padmanaban, S. (2021). Application of dynamically search space squeezed modified firefly algorithm to a novel short term economic dispatch of multi-generation systems. *IEEE Access*, 9, 1918-1939; https://doi.org/10.1109/ACCESS.2020.3046910

List of Countries by Electricity Production. In Wikipedia. [Online] Available: https://en.wikipedia.org/wiki/List_of_countries_by_electricity_production. Accessed on 1 December 2020

Ma, T., Yuan, T., Sun, Y., Chen, N., Liu, X., & Gao, B. (2017). Power generation scheduling for wind-solar-thermal power long distance consumption based on game-theory. *2017 IEEE 7th Annual International Conference on CYBER Technology in Automation, Control, and Intelligent Systems (CYBER),* Honolulu, HI, 1296-1300; https://doi.org/10.1109/CYBER.2017.8446256

Ministry of New and Renewable Energy, Government of India. Annual Report 2019-20. Available: https://mnre.gov.in/. Accessed on 27 October, 2020

Mohamed, M., Youssef, A., Ebeed, M., & Kamel, S. (2019). Hybrid optimization technique for short term wind-solar-hydrothermal generation scheduling. *IEEE Conference on Power Electronics and Renewable Energy (CPERE),* Aswan City, Egypt, pp. 212-216; https://doi.org/10.1109/CPERE45374.2019.8980237

Mondal, S., Bhattacharya, A., & Dey, S.H.N. (2013). Multi-objective economic emission load dispatch solution using gravitational search algorithm and considering wind power penetration. *International Journal of Electrical Power and Energy Systems*, 44(1), 282-292; https://doi.org/10.1016/j.ijepes.2012.06.049

Muppandal Wind Farm. In Wikipedia. [Online] Available: https://en.wikipedia.org/wiki/Muppandal_Wind_Farm. Accessed on 20 December 2020

Nagababu, G., Bavishi, D., Kachhwaha, S.S., & Savsani, V. (2015). Evaluation of wind resource in selected locations in Gujarat. *Energy Procedia,* 79, 212-219; https://doi.org/10.1016/j.egypro.2015.11.467

Narang, N., Dhillon, J.S., & Kothari, D.P. (2014). Scheduling short-term hydrothermal generation using predator prey optimization technique. *Applied Soft Computing,* 21, 298-308; https://doi.org/10.1016/j.asoc.2014.03.029

Naversen, C.Ø., Helseth, A., Li, B., Parvania, M., Farahmand, H., & Catalão, J.P.S. (2020). Hydrothermal scheduling in the continuous-time framework. *Electric Power Systems Research,* 189, 106787; https://doi.org/10.1016/j.epsr.2020.106787

NCERT India. India - Size and Location. 2020-21. [Online] Available: https://ncert.nic.in/textbook/pdf/iess101.pdf. Accessed on 10 September, 2020

Nguyen, T.T., Pham, L.H., Mohammadi, F., & Kien, L.C. (2020). Optimal scheduling of large scale wind-hydro-thermal systems with fixed-head short-term model. *Applied Sciences,* 10(8), 2964; https://doi.org/10.3390/app10082964

Panda, A., & Tripathy, M. (2016). Solution of wind integrated thermal generation system for environmental optimal power flow using hybrid algorithm. *Journal of Electrical Systems and Information Technology,* 3(2), 151-160; https://doi.org/10.1016/j.jesit.2016.01.004

Rahimi, M., Ardakani, F.J., & Ardakani, A.J. (2021). Optimal stochastic scheduling of electrical and thermal renewable and non-renewable resources in virtual power plant. *International Journal of Electrical Power & Energy Systems,* 127, 106658; https://doi.org/10.1016/j.ijepes.2020.106658

Reddy, S.S. (2017a). Optimal scheduling of wind-thermal power system using clustered adaptive teaching learning based optimization. *Electrical Engineering,* 99, 535-550; https://doi.org/10.1007/s00202-016-0382-5

Reddy, S.S. (2017b). Optimization of renewable energy resources in hybrid energy systems. *Journal of Green Engineering,* 7(1&2), 43-60; https://doi.org/10.13052/jge1904-4720.7123

Reddy, S.S., Park, J.Y., & Jung, C.M. (2016). Optimal operation of microgrid using hybrid differential evolution and harmony search algorithm. *Frontiers in Energy,* 10(3), 355-362; https://doi.org/10.1007/s11708-016-0414-x

Renewable Energy in India. In Wikipedia. [Online] Available: https://en.wikipedia.org/wiki/Renewable_energy_in_India#:~

:text=As%20of%2027%20November%202020,GW%20out%20 of%20373%20GW).&text=According%20to%202027%20blueprint%2C%20India,%E2%80%9Cother%20zero%20emission% E2%80%9D%20sources. Accessed on 10 December 2020

Saxena, B.K., & Rao, K.V.S. (2015). Comparison of Weibull parameters computation methods and analytical estimation of wind turbine capacity factor using polynomial power curve model: case study of a wind farm. *Renewables: Wind, Water, and Solar,* 2, 3; https://doi.org/10.1186/s40807-014-0003-8

Saxena, N., & Ganguli, S. (2015). Solar and wind power estimation and economic load dispatch using firefly algorithm. *Procedia Computer Science,* 70, 688-700; https://doi.org/10.1016/j.procs.2015.10.106

Singal, R.K. (2009). *Non-Conventional Energy Resources,* 2nd ed., S. K. Kataria & Sons, New Delhi, India. ISBN-8188458821

Sukkiramathi, K., & Seshaiah, C.V. (2020). Analysis of wind power potential by the three-parameter Weibull distribution to install a wind turbine. *Energy Exploration & Exploitation,* 38(1), 158-174; https://doi.org/10.1177%2F0144598719871628

Takahama, T., & Sakai, S. (2005). Constrained optimization by applying the /spl alpha/ constrained method to the nonlinear simplex method with mutations. *IEEE Transactions on Evolutionary Computation,* 9(5), 437-451; https://doi.org/10.1109/TEVC.2005.850256

Tamil Nadu Generation and Distribution Corporation Limited. www.tangedco.gov.in

Tan, S., Wang, X., & Jiang, C. (2019). Optimal scheduling of hydro-PV-Wind hybrid system considering CHP and BESS coordination. *Applied Sciences,* 9(5), 892; https://doi.org/10.3390/app9050892

Vaderobli, A., Parikh, D., & Diwekar, U. (2020). Optimization under uncertainty to reduce the cost of energy for parabolic trough solar power plants for different weather conditions. *Energies,* 13(12), 3131; https://doi.org/10.3390/en13123131